Int J Clin Exp Med 2017;10(7):10123-10132
www.ijcem.com /ISSN:1940-5901/IJCEM0046733

Original Article

Identifying RHEB as a metastatic driver in clear-cell renal cell carcinoma through bioinformatics analysis

Zhiyong Lv, Hao He, Lindong Lv, Wenbing Zhang

Urology Department of The General Hospital of Ningxia Medical University, Yinchuan, Ningxia, China

Received September 1, 2016; Accepted February 1, 2017; Epub July 15, 2017; Published July 30, 2017

Abstract: The present study was aimed to investigate the candidate genes involved in metastasis of clear-cell renal cell carcinoma (ccRCC). ccRCC tissues were collected from 36 patients with metastasis (mRCC) and 46 patients without metastasis (pRCC) and gene expressions were analyzed through RNA-Sequencing (RNA-Seq) technology. Differentially expressed genes (DEGs) were recognized via limma package (logFC>0.7 or <-0.7 and P<0.05), and protein-protein interaction (PPI) network was constructed as a DEGs connection pathway. Moreover, the analysis of pathway and function were performed through using the analysis of gene ontology (GO) enrichment and Kyoto encyclopedia of genes and genomes (KEGG) pathway. Finally, MTT and transwell assays were performed to identify the effects of selected gene in ccRCC cell *in vitro*. Through analyzing the data of RNA-Seq, it was observed that 1207 genes were differentially expressed between ccRCC tissues with or without metastasis, including 724 of down-regulation and 483 of up-regulation, and *Rheb* was selected as a candidate gene involved in ccRCC metastasis. The results indicated that *Rheb* could promote ccRCC cell proliferation, invasion and migration *in vitro*. From those it could be found *Rheb* played important roles in the metastasis of ccRCC.

Keywords: ccRCC, RNA-Seq, *Rheb*, proliferation, invasion, migration

Introduction

Renal cell carcinoma (RCC) is a highly aggressive malignancy which consists of three different pathological types, including clear-cell renal cell carcinoma (ccRCC), chromophoberenal cell carcinoma and papillary renal cell carcinoma, accounts for more than 90% of kidney cancers, and 2-3% of all adult malignancies [1, 2]. Among all pathological types of RCC, ccRCC is the most prevalent one comprising 80 to 90% of RCC cases [3]. Remarkable biological heterogeneities and varied prognosis have been reported within mRCC, therefore there is still lack of reliable biomarkers which could not be helpful to stratify ccRCC patients with the risk of metastasis [4].

It is widely accepted that microvascular invasion indicates a pro-metastatic state in various cancers [5]. During metastasis program, tumor cells undergo significant morphological changes between epithelial and mesenchymal states [6]. ccRCC is featured by specific metastatic patterns, being lungs, liver and skeletal system the most commonly affected sites. Prognosis for patients with mRCC remains greatly unfavorable, with a median survival time of eight months and 5-year survival rate of nearly 10% [7]. But the molecular effectors underlying metastasis in ccRCC remains to poorly understand.

During the last several decades, great achievements have been made in the analysis of gene expression owing to the practice of transcriptomic profiling based on high-throughput sequencing (RNA-Seq) [8, 9]. A great number of sequence with bioinformatics and experimental data from a wide inventory of human tissue specimens have contributed to recognized DEGs with subsequent applicability in clinic. However, to our knowledge, people haven't compared the difference of transcriptional profiling between ccRCC tissues with or without metastasis. Through next generation sequencing based on RNA-seq, gene expression profiling of 36 ccRCC specimens with metastasis and 46 ccRCC specimens without metastasis were collected in clinical patients.

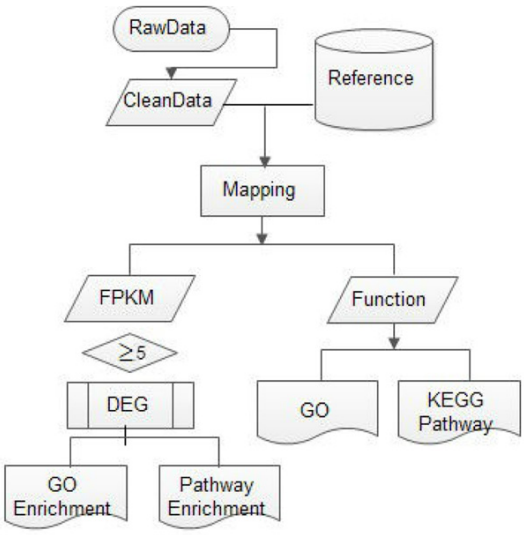

Figure 1. The schematic workflow for RNA-sequence.

Therefore, the current study aimed to identify selected genes involved in the metastasis of ccRCC through RNA-sequence and data analysis. Furthermore, we detected the effects of knockdown of relevant gene on the proliferation, invasion and migration of ccRCC cells *in vitro*.

Materials and methods

Patients and specimens

ccRCC tissue samples were acquired from randomly selected 36 patients with mRCC and 46 patients without metastasis (pRCC) during the period from March, 2014 to October, 2015 at the Department of Urology, the general Hospital of Ningxia University College of Medicine (Yinchuan, China). None of the patients had undergone any previous cancer-related therapy, or had a history of any other kinds of tumors. After operation, these fresh tissues were promptly frozen and conserved in liquid nitrogen for further use. The study got approval from the Medical Ethical Committee of the College of Medicine, Ningxia Medical University. Prior to tissue collection, all patients have been fully acquainted with the project and have signed informed consents.

Cell culture

Human ccRCC cell lines ACHN were acquired from the Cell Bank of the Institute of Biochemistry and Cell Biology, Chinese Academy of Sciences (Shanghai, China). All cell lines were cultured in DMEM (Gibco, Shanghai) with adding 10% FBS (Gibco, Shanghai) in a humidified incubator of 5% CO_2 maintained at 37°C.

RNA-sequence and data analysis

Total RNA extraction was performed using a TRIzol reagent kit (Life Technologies, Inc., Rockville, MD, USA) according to the company's specifications. SOLiD Total RNA-Seq Kit (Ambion) was used to prepare the libraries. Following library quantification, each library was plated onto a single read flow cell for sequencing on an Illumina HiSeq 2500 sequencer, generating 2×100 bp reads. The FastQC (http://www.bioinformatics.babraham.ac.uk/projects/fastqc/) was used for Quality Check and raw reads were filtered by removal of adapter and low quality reads. After stringent quality assessment and data filtering, clean reads were mapped to the human genome using Bowtie2 software (http://tophat.cbcb.umd.edu/) for evaluation of sequence alignments [10].

Differential expression analysis between mRCC and pRCC tissues (paired t-test) was performed with the limma package implemented in Bioconductor using the FPKM (Fragments PerKilobase of transcript per Million mapped reads) method [11]. Only transcripts were found to be differentially expressed with an FDR-adjusted *P*-value <0.05 (adjusted using Benjamini-Hochberg false discovery rate (FDR) procedure, and with a minimum of logFC (fold change) >0.7 or <-0.7 were considered significant and used for further analysis. GO and KEGG pathway analysis of up- and down-regulated genes were performed using DAVID (Database for Annotation, Visualization, and Integrated Discovery) Bioinformatics Resources 6.7 [12] for functional enr ichment analysis. The complete diagram of RNA-sequence was shown in **Figure 1**.

qRT-PCR

The expression levels of *Rheb* were investigated through Quantitative Real-time PCR (qRT-PCR). Synthesis of cDNAs was carried out by a reverse transcription kit (Bio-Rad, Hercules, California, USA). qRT-PCR reactions were carried out by a preheated ABI 7500 Real-Time PCR System (Applied Biosystems, Carlsbad, USA). The primer sequences used in this study were as follows: β-actin, forward: 5'-CTGGAA-

CGGTGAAGGTGAC-3' and reverse: 5'-AAGGGACTTCCTGTAACAATGC-3'; *Rheb*, forward: 5'-ACCTGCATATGGAAAGGGTG-3' and reverse: 5'-TTCCCAGTGTCCTCAGGCT-3'. The analysis of relative gene expressions should be performed at three times independently, and each sample should be verified in triplicate. Fold changes were calculated and determined using relative quantification methods ($2^{-\Delta\Delta Ct}$) [13]. β-actin was served as internal control.

Protein isolation and western blot analysis

Total protein was isolated from the cells using RIPA buffer (Beyotime, Jiangsu, China) containing protease inhibitor mixture (Beyotime). According to the manufacturer's protocol, the protein concentration was assessed through a Bradford protein assay (Bio-Rad, Hercules, CA, USA). The protein samples with equal amounts (20 μg) were then loaded onto a SDS-PAGE gel and transferred onto PVDF membranes (Amersham Biosciences, Piscataway, NJ, USA). The membranes were incubated with the specific primary antibodies overnight at 4°C. Primary antibodies were as follows: RHEB (1:1000; Abcam, USA) and GAPDH (1:5000; Abcam, USA). Membranes were then probed with appropriate HRP-conjugated secondary antibodies for 2 h at room temperature. The membranes were developed using Western chemiluminescent ECL reagent (Tiangen, Beijing, China) and exposed to X-ray film. The density of the bands on the membrane was quantified by Quantity One software (Bio-Rad Laboratories, Milan, Italy) with GAPDH as the internal control.

Plasmid construction and transfection

Human *Rheb* (NM_005614.3) mRNA sequence was obtained from NCBI Genbank. In purpose of depletion of *Rheb* to silence *Rheb* expression, a pair of *Rheb*-short hairpin RNA (shRNA) oligonucleotides were chemically synthesized, annealed and constructed into the pSuper-retro-puro-vector (Oligoengine, Seattle, WA, USA) as sh*Rheb* [14]. Scramble shRNA was inserted into the pSuper-retro-puro-vector as shCon. sh*Rheb* or shCon was transfected into ACHN cells using Lipofectamine 2000 reagent (Invitrogen) in accordance to the manufacturer's instructions. 48 h after transfection, puromycin (1 μg/mL) was used to screen and establish stable ACHN cells expressing sh*Rheb* or shCon.

Cell proliferation assay

The *in vitro* proliferation of ACHN cells were measured by MTT assay (Sigma, St. Louis, MO, USA). ACHN cells were seeded into 96-well plates in a density of 1×10^4 cells/well. After 1, 2, 3, 4 and 5 days of transfection, culture medium was replaced with fresh medium containing MTT dye (20 μL/well) and incubated with the cells for another 4 h. After supernatant removal, DMSO (150 μl/well; Sigma, USA) was added and thoroughly mixed for 15 minutes. The absorbance value at 450 nm was measured by Universal Microplate Spectrophotometer (Bio-Tek Instruments, Inc., Winooski, USA).

Cell transwell assays

24-well transwell chambers (Costar, Corning, Switzerland) with uncoated or Matrigel-coated membranes were respectively used for migration and invasion assays in this research. Briefly, the post-transfected ACHN cells were seeded onto the upper chamber contained serum-free medium, while medium supplemented with 10% FBS acted as chemoattractant was added to the lower chamber. After incubation for 16 hours (migration assay) or 24 hours (invasion assay), cells which did not migrated across the upper surface were removed with cotton swabs, while cells which adhered to the lower surface of the inserts were stained with 0.1% crystal violet for 20 minutes. Finally the whole filters were washed twice in water and observed.

Statistical analysis

All statistical analysis of this research was performed using SPSS 17.0 (IBM, Chicago, IL, USA) and GraphpadPrism 5.0 (Graphpad Software, San Diego, CA, USA). All the results of *in vitro* trials were addressed as mean ± SD (standard deviation) from three separate experiments in triplicates, and the data was further analyzed using double-sided Student's *t*-test. $P<0.05$ was regarded to indicate a statistically significant result in this research.

Results

RNA-sequence and data analysis

According to different clinical phenotypes, the patients were subsequently divided into two

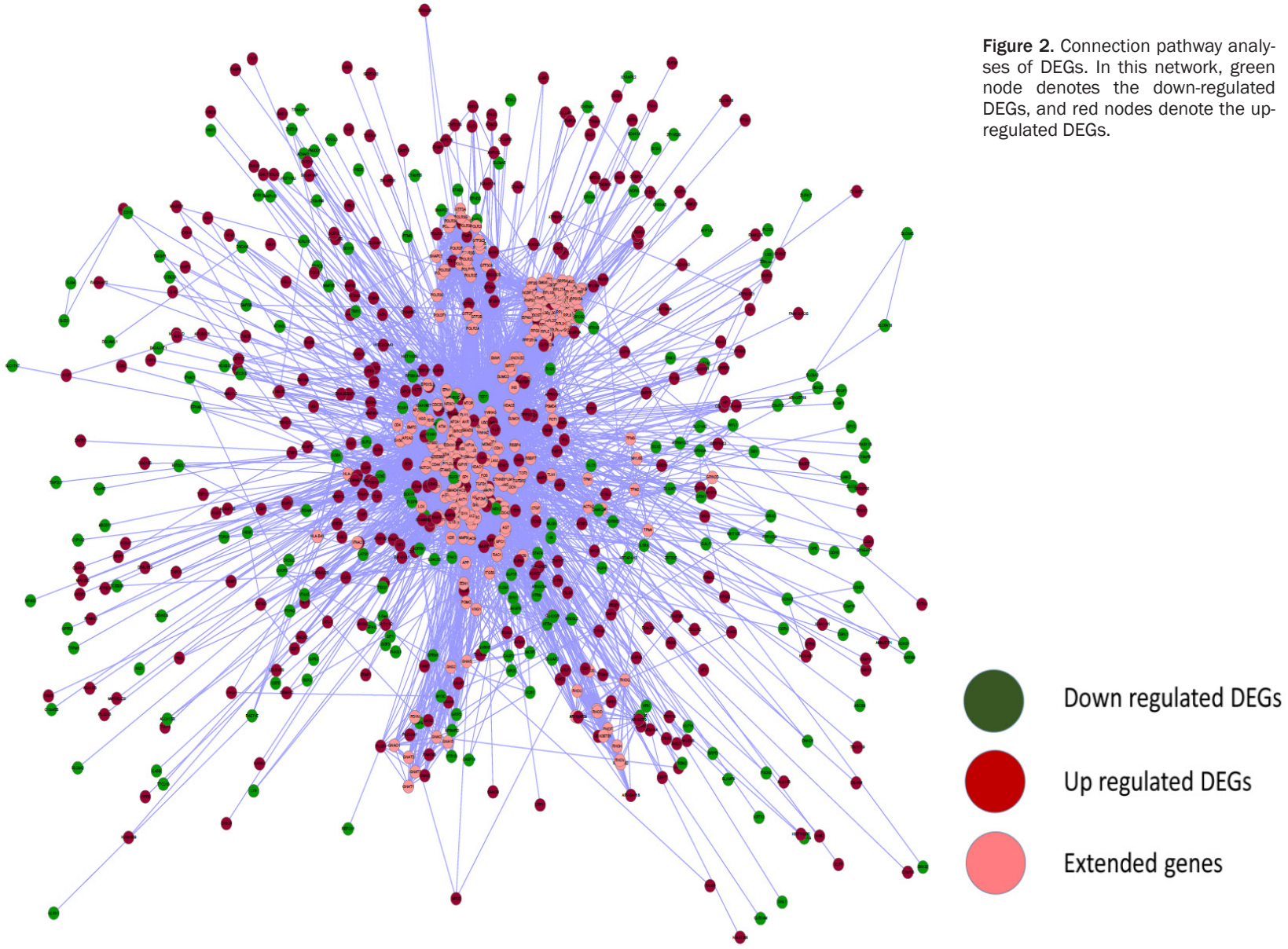

Figure 2. Connection pathway analyses of DEGs. In this network, green node denotes the down-regulated DEGs, and red nodes denote the up-regulated DEGs.

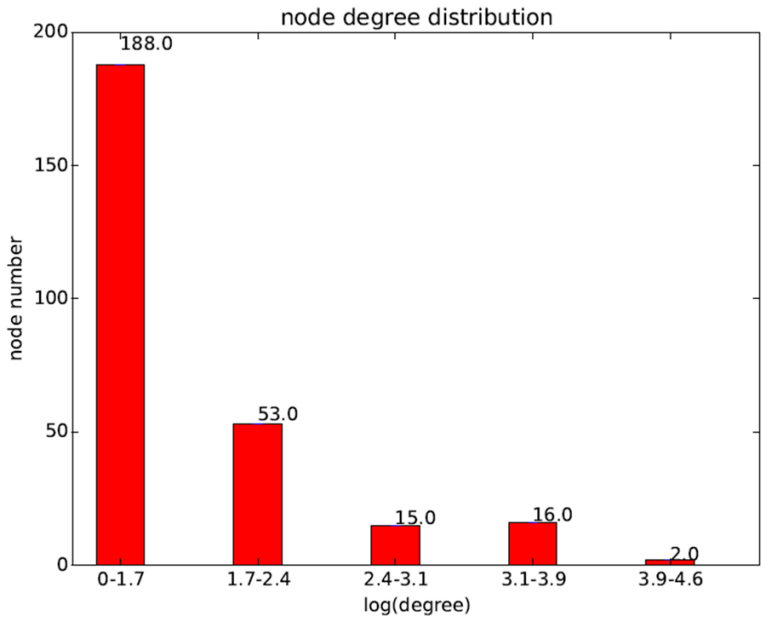

Figure 3. DEGs degree distribution.

groups, including 36 samples of mRCC and 46 samples of pRCC. All the genetic IDs have been transferred into a gene symbol. Limma algorithm was conducted based on the difference of genes expression between two groups, and 1207 genes have been selected and collected, including 724 of down-regulation and 483 of up-regulation, according to the logFC>0.7 or <-0.7 and P<0.05 as a significant threshold.

In order to analysis the DEGs in the protein-protein interaction (PPI) network, and to find the ways these genes to interact with others to affect the transfer capacity of ccRCC, the integration of the interaction between genes was constructed through the STRING database [15] as a DEGs connection pathway. The network nodes of DEGs, and their expansion and extension through the connection pathway of interaction provided us with at least 20 DEGs which have direct interactions with other genes in the connection pathway, as shown in **Figure 2**.

Identification and functional analysis of 100 DEGs

Through the analysis of the connection pathway, the network node degree distribution of the DEGs was measured, which was demonstrated in **Figure 3**.

Using unsupervised clustering algorithm, it was confirmed the top 100 genes which could be used to effectively distinguish metastatic carcinoma from non-metastatic carcinoma. The heat-map of 100 differentially expressed genes was present in **Figure 4**. The top 100 genes were submitted to pathway and function analysis using the GO enrichment and KEGG pathway analysis, and all the data were recorded in Tables S1 and S2.

Rheb gene analysis

Finding the diagnostic markers which can be used to predict the metastasis risks of ccRCC patients from these top 100 genes, the genes were characterized and their expressions in the sample were used as the characteristic value, combined with the recursive feature elimination algorithm for further feature selection, then the results was obtained as illustrated in **Figure 5**. It was found that when the 15 features were combined, the highest model prediction accuracy can be achieved at approximately 85%, which was marked red in the figure. And the selected 15 features (genes) were recorded in **Table 1**. *Rheb*, as a candidate of 15 genes, had been previously reported to be closely correlated to the metastasis of kidney cancer [16]. Subsequently, KEGG pathway analysis was performed to explore the relative pathway of *Rheb*, which were presented in **Table 2**.

Rheb could promote ccRCC cell proliferation, invasion and migration

As the previous results showed that *Rheb* might be a valuable candidate, its role in ccRCC cells was further validated. *Rheb* expression of ACHN cells transfected with sh*Rheb* reduced greatly than controls revealed by both qRT-PCR and western blot (**Figure 6A**, P<0.05). Whether *Rheb* could affect cell proliferation was verified through conducting MTT growth assay over a five-day period. As demonstrated in **Figure 6B**, sh*Rheb* was found to significantly repress cell proliferation (P<0.05), which indicated that *Rheb* expression was significantly associated with ccRCC proliferation. Furthermore, we could uncover that the migration and

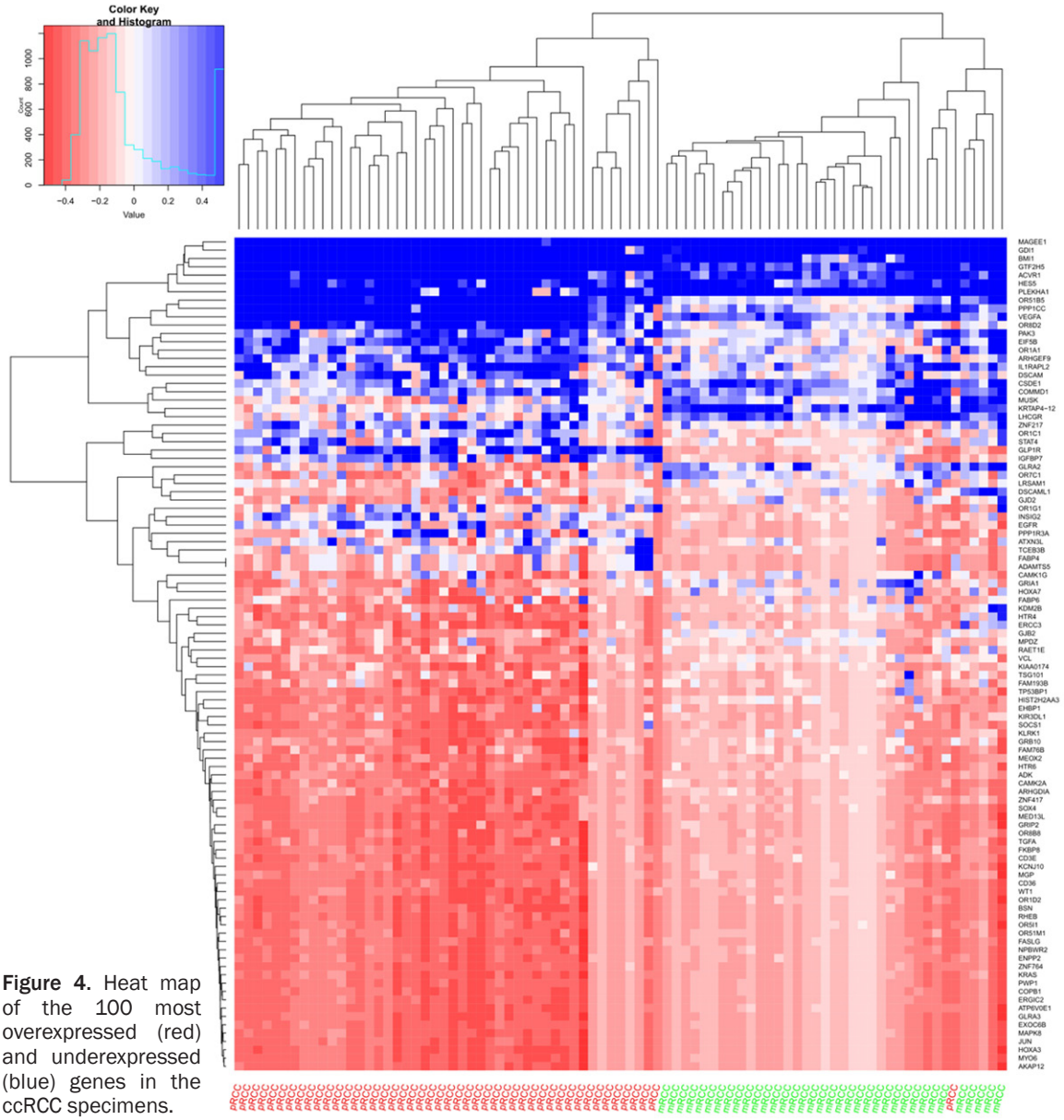

Figure 4. Heat map of the 100 most overexpressed (red) and underexpressed (blue) genes in the ccRCC specimens.

invasion capacities of sh*Rheb* cells were dramatically inhibited compared to the controls, revealed by transwell assays ($P<0.05$; **Figure 6C** and **6D**). And the cells with sh*Rheb* transfected showed a sharply decrease in cell invasion and migration ability. Collectively, the results mentioned above presented a clear conclusion that down-expression of *Rheb* could suppress ccRCC cell proliferation, invasion and migration *in vitro*.

Discussion

In this study, through analyzing the data of RNA-seq, it was indicated that Ras homolog enriched in brain (*Rheb*) might be a promising biomarker for the metastasis of ccRCC. Then, the further investigations were identified that *Rheb* could promote ccRCC cells proliferation, invasion and migration*in vitro*. The present research is the result of candidate genes discovery in clinical ccRCC tissue through RNA-seq.

Although protein pattern could only be partially illustrated by mRNA concentration [17], mRNA expression was clearly an indicator for protein expression. Recent studies suggested that RNA-Seq provided a great deal of transcriptional detail in comparison to genome-wide micro-

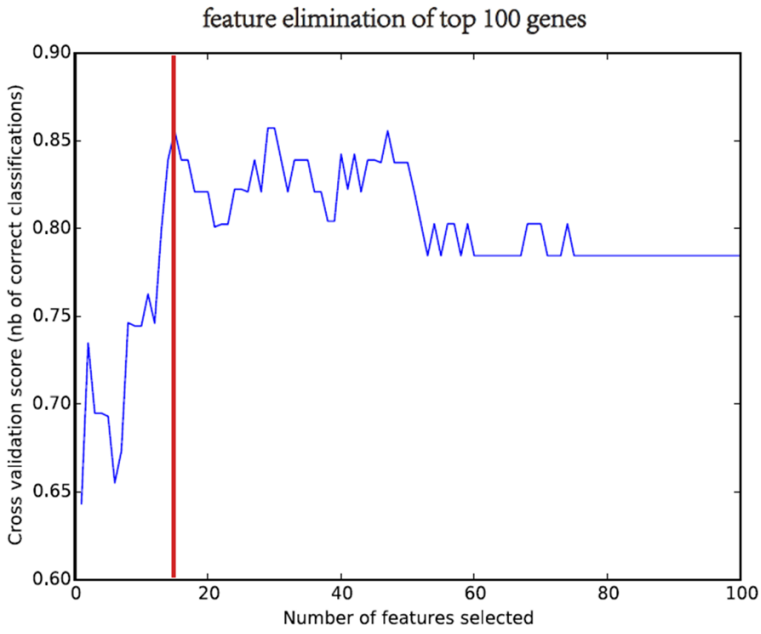

Figure 5. Feature selected of top 100 genes.

Table 1. Selected 15 genes

Gene	logFC	*P* value	Cancer type
Hes5	-0.89248	0.0018484	Breast cancer
Znf417	-0.82599	0.0039565	Prostate cancer
Glr2	-0.98549	0.0005859	-
Or8d2	-0.81352	0.0045381	-
Hoxa7	0.714953	0.0126229	Breast cancer
Fabp6	0.923417	0.0012752	Colorectal cancer
Musk	-0.79751	0.0053985	-
Htr6	-0.76513	0.007601	-
Grip2	-0.99734	0.0005026	-
Or51m1	-0.81252	0.0045881	-
Or1c1	-0.77549	0.0068216	-
Klrk1	-0.9248	0.0012539	-
Vegfa	0.84416	0.0032296	Kidney cancer metastasis
Akap12	0.97641	0.0006583	-
Rheb	0.92876	0.0011947	Kidney cancer metastasis

arrays, especially for investigating low-copy transcripts and that it provided for an overall up-regulated dynamic range of signal intensity at 2 to 3 orders of magnitude greater than microarrays [18, 19]. Therefore RNA-seqwas quite suited for the research of both known and novel transcript isoforms.

It was known that most DNA mutations might had relationships with ccRCC metastasis, according to the present results and previous researches, many genes which might be implicated in the development of ccRCC should be identified using the latest technology. That was the reason we performed the experiments using tumor tissue with or without metastasis. And actually we found some interesting genes that may have important role comparing the RNA-seq data between these two sets. Results indicated that *Rheb* played important roles in ccRCC metastasis.

Metastasis of ccRCC commonly indicated the poor progression, including low 5-year survival rate [20], unfavorable quality of life and ineffective treatment [21]. Of note, a great number of studies were related to the ccRCC metastasis. For example, Zhang et al. [22] demonstrated that expression of long non-coding RNA MALAT1 was significantly up-regulated in ccRCC tissues and RCC cell lines and silencing of long non-coding RNA MALAT1 suppressed ccRCC cell proliferation, migration and invasion. However, the entire mechanism of ccRCC metastasis remained to be further elucidated.

RHEB, as a protein of the Ras superfamily GTPases of 21 kDa, served as an upstream activator of mTORC1 (mammalian target of rapamycin complex 1) [23, 24]. Previous studies had indicated that RHEB-mTORC1 might be an important signaling axis in mediating a variety of cellular activities in accordance with environmental nutrient availability [25, 26]. Activity status of *Rheb* could repress mTORC2 and PI3K pathway by inducing multiple mTORC1-dependent negative feedback loops [27]. *Rheb*, originally identified in brain neurons [23], was also found to be overexpressed in a wide variety of human cancers, such as hepatic cancer [28], ovarian cancer [29], renal cell carcinoma [30] and acute myelogenous leukemia [31].

Table 2. GO enrichment and KEGG pathway analysis of *Rheb* gene

Category	ID	Terms	*P* value	Ratio (%)
GOTERM_BP_5	GO:0007242	Intracellular signaling cascade	0.032	16
KEGG_PATHWAY	hsa04910	Insulin signaling pathway	0.011	6

Ratio = number of DEGs mapped to the pathway/total number of genes of the pathway.

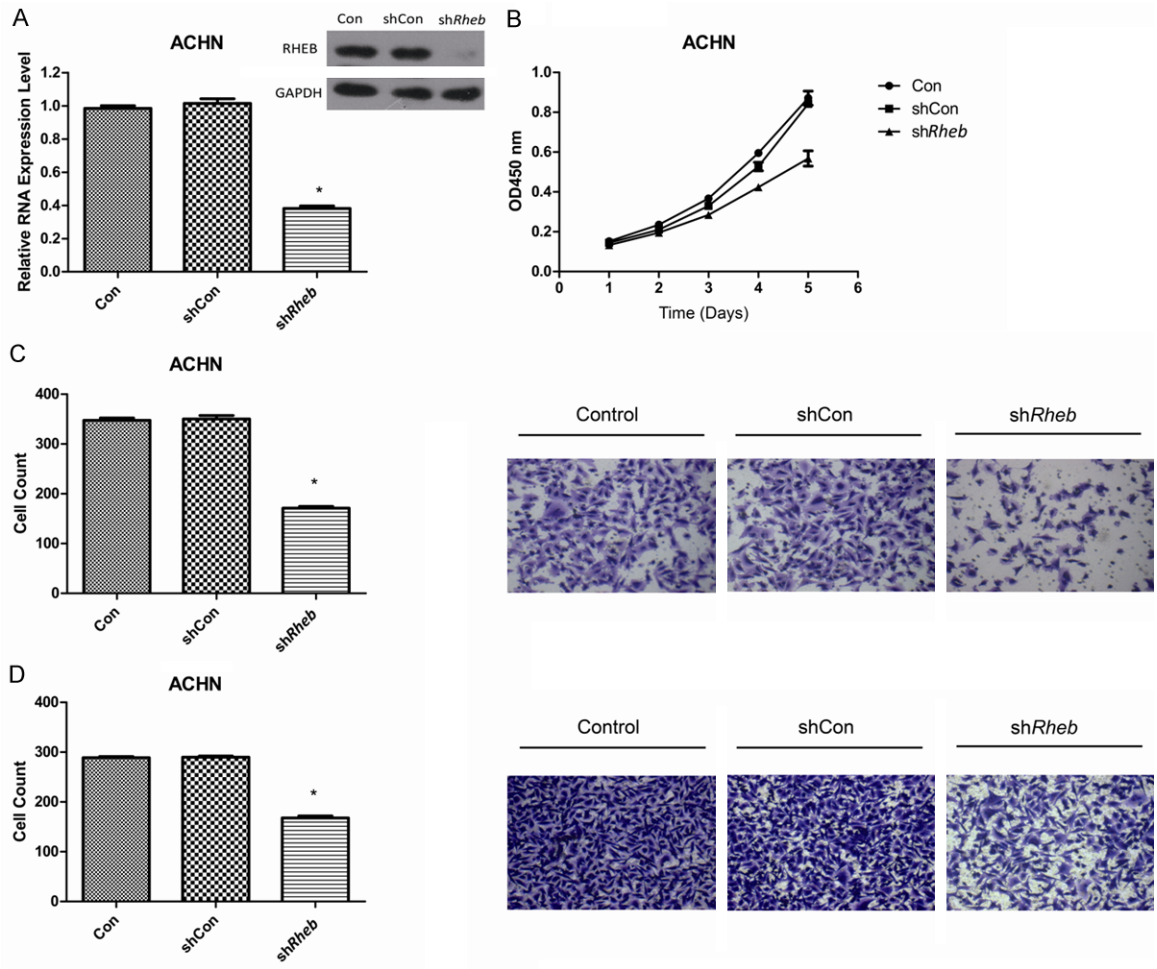

Figure 6. Silencing *Rheb* inhibits ACHN cell proliferation, invasion and migration *in vitro*. (A) RHEB mRNA and protein levels in ACHN cells after transfection with shCon and sh*Rheb* were detected using qRT-PCR and western blot. (B) ACHN cell proliferation was measured by MTT assay. ACHN cell invasion (C) and migration (D) capacities were investigated after transfection as indicated previously. Data are presented as mean ± SD (standard deviation). **P*<0.05 vs. shCon.

Moreover, in non-small cell lung cancer cells, RHEB might be a key molecule for farnesyltransferase inhibitors (FTIs) therapy [32]. In addition, emerging evidence revealed that *Rheb* was associated with the metastasis of RCC [16]. Consistently, in the current research, we revealed that *Rheb* could promote ccRCC cell proliferation, invasion and migration *in vitro*.

Actually, in this study, we only tested and verified the metastatic role of *Rheb* in a ccRCC cell lines and we did not clarify the specific mechanism how *Rheb* could affect the metastasis of ccRCC. Therefore, based on the present study, we would devote into exploring and clarifying the interaction between *Rheb* and its downstream target and the underlying mechanism how *Rheb* could promote the metastasis of ccRCC in further study.

In conclusion, the genes found in the present study provided us a lot of information and suggestions which may lead us to get much closer

to dealing with the problems of ccRCC metastasis we are facing. Among them, *Rheb* gene could promote the proliferation, invasion and migration of ccRCC cells *in vitro*, which could be considered as a promising target for diagnosis and treatment of ccRCC metastasis in the near future.

Acknowledgements

The work of our research was supported by Natural Science Foundation of Ningxia (Grant number: NZ14115).

Disclosure of conflict of interest

None.

Address correspondence to: Dr. Zhiyong Lv, Urology Department of The General Hospital of Ningxia Medical University, 804 Shengli Street, Xingqing Area, Yinchuan, Ningxia, China. Tel: +86-139950-13663; Fax: +86-0951-6743248; E-mail: Zhiyong-0082@126.com

References

[1] Rini BI, Campbell SC and Escudier B. Renal cell carcinoma. Lancet 2009; 373: 1119-1132.

[2] Escudier B, Porta C, Schmidinger M, Algaba F, Patard JJ, Khoo V, Eisen T, Horwich A; ESMO Guidelines Working Group. Renal cell carcinoma: ESMO clinical practice guidelines for diagnosis, treatment and follow-up. Ann Oncol 2014; 25 Suppl 3: iii49-56.

[3] Lam JS, Shvarts O, Leppert JT, Figlin RA and Belldegrun AS. Renal cell carcinoma 2005: new frontiers in staging, prognostication and targeted molecular therapy. J Urol 2005; 173: 1853-1862.

[4] Jonasch E, Futreal PA, Davis IJ, Bailey ST, Kim WY, Brugarolas J, Giaccia AJ, Kurban G, Pause A, Frydman J, Zurita AJ, Rini BI, Sharma P, Atkins MB, Walker CL and Rathmell WK. State of the science: an update on renal cell carcinoma. Mol Cancer Res 2012; 10: 859-880.

[5] Kroeger N, Rampersaud EN, Patard JJ, Klatte T, Birkhauser FD, Shariat SF, Lang H, Rioux-Leclerq N, Remzi M, Zomorodian N, Kabbinavar FF, Belldegrun AS and Pantuck AJ. Prognostic value of microvascular invasion in predicting the cancer specific survival and risk of metastatic disease in renal cell carcinoma: a multicenter investigation. J Urol 2012; 187: 418-423.

[6] Nieto MA. Epithelial plasticity: a common theme in embryonic and cancer cells. Science 2013; 342: 1234850.

[7] Lin JA, Fang SU, Su CL, Hsiao CJ, Chang CC, Lin YF and Cheng CW. Silencing glucose-regulated protein 78 induced renal cell carcinoma cell line G1 cell-cycle arrest and resistance to conventional chemotherapy. Urol Oncol 2014; 32: 29, e1-11.

[8] Mane SP, Evans C, Cooper KL, Crasta OR, Folkerts O, Hutchison SK, Harkins TT, Thierry-Mieg D, Thierry-Mieg J and Jensen RV. Transcriptome sequencing of the microarray quality control (MAQC) RNA reference samples using next generation sequencing. BMC Genomics 2009; 10: 264.

[9] Xiong Y, Chen X, Chen Z, Wang X, Shi S, Zhang J and He X. RNA sequencing shows no dosage compensation of the active X-chromosome. Nat Genet 2010; 42: 1043-1047.

[10] Langmead B, Trapnell C, Pop M and Salzberg SL. Ultrafast and memory-efficient alignment of short DNA sequences to the human genome. Genome Biol 2009; 10: R25.

[11] Trapnell C, Williams BA, Pertea G, Mortazavi A, Kwan G, van Baren MJ, Salzberg SL, Wold BJ and Pachter L. Transcript assembly and quantification by RNA-Seq reveals unannotated transcripts and isoform switching during cell differentiation. Nat Biotechnol 2010; 28: 511-515.

[12] Huang da W, Sherman BT and Lempicki RA. Systematic and integrative analysis of large gene lists using DAVID bioinformatics resources. Nat Protoc 2009; 4: 44-57.

[13] Livak KJ and Schmittgen TD. Analysis of relative gene expression data using real-time quantitative PCR and the 2(-Delta Delta C(T)) Method. Methods 2001; 25: 402-408.

[14] Brummelkamp TR, Bernards R and Agami R. A system for stable expression of short interfering RNAs in mammalian cells. Science 2002; 296: 550-553.

[15] Szklarczyk D, Franceschini A, Kuhn M, Simonovic M, Roth A, Minguez P, Doerks T, Stark M, Muller J, Bork P, Jensen LJ and von Mering C. The STRING database in 2011: functional interaction networks of proteins, globally integrated and scored. Nucleic Acids Res 2011; 39: D561-568.

[16] Yalniz Z, Tigli H, Sanli O, Dalay N and Buyru N. Novel mutations and role of the LKB1 gene as a tumor suppressor in renal cell carcinoma. Tumour Biol 2014; 35: 12361-12368.

[17] Vogel C, Abreu Rde S, Ko D, Le SY, Shapiro BA, Burns SC, Sandhu D, Boutz DR, Marcotte EM and Penalva LO. Sequence signatures and mRNA concentration can explain two-thirds of protein abundance variation in a human cell line. Mol Syst Biol 2010; 6: 400.

[18] Su Z, Li Z, Chen T, Li QZ, Fang H, Ding D, Ge W, Ning B, Hong H, Perkins RG, Tong W and Shi L.

Comparing next-generation sequencing and microarray technologies in a toxicological study of the effects of aristolochic acid on rat kidneys. Chem Res Toxicol 2011; 24: 1486-1493.

[19] Chen KD, Chang PT, Ping YH, Lee HC, Yeh CW and Wang PN. Gene expression profiling of peripheral blood leukocytes identifies and validates ABCB1 as a novel biomarker for Alzheimer's disease. Neurobiol Dis 2011; 43: 698-705.

[20] Staehler MD, Kruse J, Haseke N, Stadler T, Roosen A, Karl A, Stief CG, Jauch KW and Bruns CJ. Liver resection for metastatic disease prolongs survival in renal cell carcinoma: 12-year results from a retrospective comparative analysis. World J Urol 2010; 28: 543-547.

[21] Oudard S, Medioni J, Aylllon J, Barrascourt E, Elaidi RT, Balcaceres J and Scotte F. Everolimus (RAD001): an mTOR inhibitor for the treatment of metastatic renal cell carcinoma. Expert Rev Anticancer Ther 2009; 9: 705-717.

[22] Zhang HM, Yang FQ, Chen SJ, Che J and Zheng JH. Upregulation of long non-coding RNA MALAT1 correlates with tumor progression and poor prognosis in clear cell renal cell carcinoma. Tumour Biol 2015; 36: 2947-2955.

[23] Yamagata K, Sanders LK, Kaufmann WE, Yee W, Barnes CA, Nathans D and Worley PF. rheb, a growth factor- and synaptic activity-regulated gene, encodes a novel Ras-related protein. J Biol Chem 1994; 269: 16333-16339.

[24] Inoki K, Li Y, Xu T and Guan KL. Rheb GTPase is a direct target of TSC2 GAP activity and regulates mTOR signaling. Genes Dev 2003; 17: 1829-1834.

[25] Babcock JT and Quilliam LA. Rheb/mTOR activation and regulation in cancer: novel treatment strategies beyond rapamycin. Curr Drug Targets 2011; 12: 1223-1231.

[26] Wazir U, Newbold RF, Jiang WG, Sharma AK and Mokbel K. Prognostic and therapeutic implications of mTORC1 and Rictor expression in human breast cancer. Oncol Rep 2013; 29: 1969-1974.

[27] Howell JJ and Manning BD. mTOR couples cellular nutrient sensing to organismal metabolic homeostasis. Trends Endocrinol Metab 2011; 22: 94-102.

[28] Zheng M, Zang S, Xie L, Fang X, Zhang YU, Ma X, Liu J, Lin D and Huang A. Rheb phosphorylation is involved in p38-regulated/activated protein kinase-mediated tumor suppression in liver cancer. Oncol Lett 2015; 10: 1655-1661.

[29] Altman MK, Alshamrani AA, Jia W, Nguyen HT, Fambrough JM, Tran SK, Patel MB, Hoseinzadeh P, Beedle AM and Murph MM. Suppression of the GTPase-activating protein RGS10 increases Rheb-GTP and mTOR signaling in ovarian cancer cells. Cancer Lett 2015; 369: 175-183.

[30] Ghosh AP, Marshall CB, Coric T, Shim EH, Kirkman R, Ballestas ME, Ikura M, Bjornsti MA and Sudarshan S. Point mutations of the mTOR-RHEB pathway in renal cell carcinoma. Oncotarget 2015; 6: 17895-17910.

[31] Ding H, McDonald JS, Yun S, Schneider PA, Peterson KL, Flatten KS, Loegering DA, Oberg AL, Riska SM, Huang S, Sinicrope FA, Adjei AA, Karp JE, Meng XW and Kaufmann SH. Farnesyltransferase inhibitor tipifarnib inhibits Rheb prenylation and stabilizes Bax in acute myelogenous leukemia cells. Haematologica 2014; 99: 60-69.

[32] Zheng H, Liu A, Liu B, Li M, Yu H and Luo X. Ras homologue enriched in brain is a critical target of farnesyltransferase inhibitors in non-small cell lung cancer cells. Cancer Lett 2010; 297: 117-125.

Table S1. GO enrichment analysis of the 100 DEGs

Name	Ratio (%)	*P* value
Cell surface receptor linked signal transduction	29	5.93E-05
G-protein coupled receptor protein signaling pathway	19	0.000865
Positive regulation of cellular biosynthetic process	14	0.001118
Positive regulation of biosynthetic process	14	0.001276
Positive regulation of cell communication	9	0.002423
Positive regulation of cell proliferation	10	0.002782
Regulation of cellular biosynthetic process	34	0.003083
Blood vessel morphogenesis	7	0.004015
Positive regulation of signal transduction	8	0.005168
Sensory organ development	7	0.00596
Positive regulation of nitrogen compound metabolic process	12	0.006091
Organ morphogenesis	11	0.0069
Blood vessel development	7	0.008202
Skeletal system morphogenesis	5	0.008472
Vasculature development	7	0.009181
Positive regulation of cellular metabolic process	14	0.009539
Enzyme linked receptor protein signaling pathway	8	0.011232
Sensory perception	13	0.012453
Development of primary sexual characteristics	5	0.013006
Positive regulation of macromolecule biosynthetic process	11	0.018174
Positive regulation of transcription	10	0.019307
Regulation of nucleobase, nucleoside, nucleotide and nucleic acid metabolic process	30	0.019584
Synaptic transmission	7	0.01993
Positive regulation of transcription, DNA-dependent	9	0.020718
Regulation of macromolecule biosynthetic process	30	0.021079
Angiogenesis	5	0.021586
Positive regulation of RNA metabolic process	9	0.021658
Regulation of signal transduction	13	0.022164
Regulation of transcription	28	0.022852
Positive regulation of gene expression	10	0.022907
Second-messenger-mediated signaling	6	0.026626
Regulation of apoptosis	12	0.028005
Regulation of programmed cell death	12	0.029827
Intracellular signaling cascade	16	0.03234
Positive regulation of nucleobase, nucleoside, nucleotide and nucleic acid metabolic process	10	0.034134
Embryonic organ development	5	0.034854
Regulation of gene expression	29	0.040377
Negative regulation of apoptosis	7	0.041278
Negative regulation of programmed cell death	7	0.043695
Negative regulation of cell death	7	0.044189
Tissue development	10	0.047969

Table S2. The KEGG pathway analysis of the 100 DEGs

Name	Ratio (%)	*P* value
ErbB signaling pathway	7	0.000205
Olfactory transduction	11	0.003774
Renal cell carcinoma	5	0.005057
Pancreatic cancer	5	0.005591
Neurotrophin signaling pathway	6	0.007622
Insulin signaling pathway	6	0.010807
Neuroactive ligand-receptor interaction	8	0.013084
Focal adhesion	7	0.014472
GnRH signaling pathway	5	0.016229
Natural killer cell mediated cytotoxicity	5	0.043391

Ratio = number of DEGs mapped to the pathway/total number of genes of the pathway.